Catalysis Today 244 (2015) 115–121

Contents lists available at ScienceDirect

Catalysis Today

journal homepage: www.elsevier.com/locate/cattod

Angular distributions and rovibrational excitation of N_2 molecules recombined on N-covered Ag(1 1 1) by the Eley–Rideal mechanism

J.I. Juaristi[a,b,c], E. Díaz[c], G.A. Bocan[d], R. Díez Muiño[b,c], M. Alducin[b,c], M. Blanco-Rey[a,c,*]

[a] Departamento de Física de Materiales, Facultad de Químicas UPV/EHU, Apartado 1072, 20080 Donostia-San Sebastián, Spain
[b] Centro de Física de Materiales CFM/MPC (CSIC-UPV/EHU), Paseo Manuel de Lardizabal 5, 20018 Donostia-San Sebastián, Spain
[c] Donostia International Physics Center, Paseo Manuel de Lardizabal 4, 20018 Donostia-San Sebastián, Spain
[d] CONICET and Centro Atómico Bariloche (CNEA), Av. Bustillo 9500, 8400 S.C. de Bariloche, Argentina

ARTICLE INFO

Article history:
Received 21 March 2014
Received in revised form 6 June 2014
Accepted 25 June 2014
Available online 25 July 2014

Keywords:
Gas–surface dynamics
Eley–Rideal
Potential energy surface
Molecular beams
Atomic N
N_2

ABSTRACT

Former calculations showed that atomic N incident at energies of a few eV on N-covered Ag(1 1 1) forms N_2 molecules by the Eley–Rideal (ER) mechanism, i.e. by direct pick-up of adsorbates. Here, we calculate the azimuthal angle distributions and the rovibrational energies of those ER products. We observe a non-trivial angle dependence that may result in very low in-plane ER yield for some given incident azimuthal angles. We find that most of the energy released upon N—N bond formation, about 7 eV, is stored in the rovibrational degrees of freedom independently of the incidence energy considered.

1. Introduction

It is well established that the presence of a surface, typically metallic, may energetically favour bond breaking or forming. The time scales of some of those elementary processes may, however, undermine the performance of the surface as a catalyst. For example, a usual rate-limiting step is the blocking of surface active sites by the reaction by-products, which is known as catalyst poisoning. A long-lasting efficient surface catalyst must have the ability to replenish those active sites by recombination and subsequent desorption of molecules [1].

The adsorbed species that acquire thermal excitation are likely to collide and react. This molecule formation mechanism is known as Langmuir–Hinshelwood (LH). Also important for the catalytic properties of surfaces are the recombination mechanisms that involve a gas-phase species (projectile) and an adsorbed species, namely hot-atom (HA) and Eley–Rideal (ER). In an ER reaction the adsorbate is directly picked-up by the projectile, while in the HA mechanism the projectile undergoes a few rebounds on the surface prior to the reactive collision. Experiments on recombination of gas-phase neutral species have traditionally involved light projectiles (H,D) [2–7], and later theoretical studies have revealed that the number of ER events is usually much smaller than that of HA events [8–13], with very few exceptions [14,15]. Recombination of heavier species, from O-atom beams for example, has been mostly attributed to the LH mechanism [16–19]. Recently, however, a highly efficient ER channel for N_2 formation has been found on Ag(1 1 1) for N-atom beams [20,21]. This reaction is the focus of the present paper.

A fundamental question in the dynamics of chemical reactions is how the total energy available in the system is shared among the different degrees of freedom of the product. This topic is not specific of reactions on surfaces, but it has also been studied in the gas phase using crossed molecular beams. In this area, the models proposed to describe the energy partitioning have considered interaction potentials as well as linear and angular momentum conservation conditions [22,23].

In the case of reactions on surfaces, the energy partitioning is mostly determined by the multidimensionality of the potential energy surface (PES) that describes the gas/surface interaction, though the energy exchange with the surface is another ingredient that needs to be considered. The molecules formed by LH recombination of adsorbates typically desorb at directions close to the

* Corresponding author at: Departamento de Física de Materiales, Facultad de Químicas UPV/EHU, Apartado 1072, 20080 Donostia-San Sebastián, Spain.
Tel.: +34 943015366.
E-mail addresses: wapalocm@ehu.es (M. Alducin), maria.blanco@ehu.es (M. Blanco-Rey).

http://dx.doi.org/10.1016/j.cattod.2014.06.028
0920-5861/

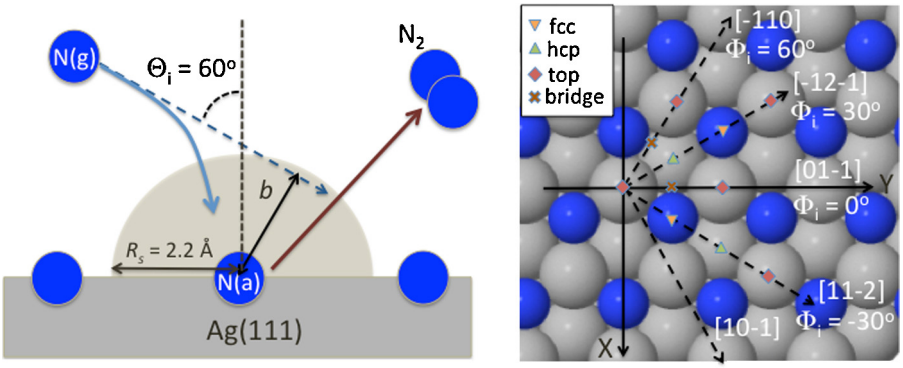

Fig. 1. Left panel: the straight dashed arrow shows the incidence direction of N(g) atoms with impact parameter *b*. The semi-spherical shaded region around N(a) with radius R_s = 2.2 Å corresponds to the area where the 6D PES is used in the simulation. The curved solid blue arrow depicts a typical atomic trajectory that undergoes deflection by the 3D attractive PES. Right panel: top view of the N-covered Ag(1 1 1) surface, with N(a) atoms occupying the fcc adsorption sites. The dashed arrows show the incident azimuthal angles (and corresponding crystallographic directions) discussed in the main text. (For interpretation of the references to colour in this figure legend, the reader is referred to the web version of this article.)

surface normal and tend to be in low lying rovibrationally excited states. The characterisation of these molecules can be used to map the transition states and other PES features, as well as to make predictions on the conditions leading to dissociative adsorption, i.e. the inverse process to associative desorption [24]. For example, it is observed that N_2 desorbs from Cu(1 1 1) [25] and Ag(1 1 1) [26] carrying hyperthermal translational and internal energies that seem consistent with the different activation barriers of those systems.

Upon recombination by the HA and ER mechanisms highly rovibrationally excited products are retrieved. The molecules formed by these mechanisms desorb with off-normal angular distributions and translational energies that increase for increasing incident projectile energies, E_i, due to partial conservation of the momentum. It is not easy to predict energy partitioning in HA and ER recombination scenarios. The aforementioned factors, such as the PES topography and the energy exchange with the surface, together with the incidence conditions of the gas-phase species, make the energy partitioning details highly dependent on the particular system under study. For this reason, accurate ab-initio modelling and molecular dynamics (MD) simulations are needed to understand the wide range of behaviours described in the literature on ER and HA processes. On Cl-covered Au(1 1 1), for example, highly vibrationally excited HCl formation is reported by experiments due to the attractive potential, but it has been suggested that a fraction of the energy may be diverted into electron–hole (e–h) pair excitations [10,13,27]. This dissipation channel is, indeed, highly effective for HAs moving on the surface [28]. It is a commonly observed trend in simulations of ER that the product shows larger rovibrational energies for larger E_i values. This has been obtained, for example, for H_2 on W(1 0 0) [15], N_2 on W(1 0 0) [29,30] and CO on Pt(1 1 1) [31]. The ER route for H_2 formation on graphene shows a much more complex dependence with E_i. Physisorbed H atoms lead to vibrationally hotter molecules than chemisorbed ones, while rotational and translational components have similar behaviours [32,33].

The focus of the present work is N_2 formed on N-covered Ag(1 1 1), a case of highly efficient direct ER recombination at high E_i values. It was found in a series of molecular beam experiments by Kleyn and co-workers on N_2 scattering off clean and N-covered Ag(1 1 1) that a fraction of the detected molecules could not be explained by reflection [20]. Instead, it was proposed that the N-atoms present in the incident beam react with the adsorbed ones [20,34]. By means of three-dimensional (3D) and six-dimensional (6D) PESs constructed from ab-initio data and MD simulations, we have shown in a previous work that an ER mechanism is at work, with an efficiency of around 35% at the experimental range of incident atom energies, which have an average value $\langle E_i \rangle$=4.3 eV, and high coverage, Θ = 1 [21]. We note that the 35% ER efficiency found in Ref. [21] sets a lower boundary for the total N_2 yield in this system. The N-atoms that do not succeed to undergo an ER reaction, which are not considered in the simulations, may still produce N_2 molecules by HA or LH at the given coverage Θ = 1. The aforementioned ER efficiency value is equivalent to cross-sections $\sigma > 2.5$ Å, larger than $\sigma = 0.4$ Å found for the same reaction on W(1 0 0) [29]. The long-range attractive and barrierless potential experienced by the N-atoms when approaching the surface is responsible for the high efficiency, and a similar behaviour is expected for other systems with these PES features [21]. In fact, recent experiments by Kleyn and co-workers for N scattering off N-covered Ru(0 0 0 1) suggest that a fast recombination channel is present [35]. On the contrary, lower efficiencies are expected for N_2 formed by ER on W(1 0 0), where an energy barrier is experienced by the approaching N-atom [29,30]. Since scattered molecules usually show lower excited internal states, the aforementioned ER and HA product properties can be used as an additional criterion to identify the recombined molecules.

In the present paper we characterise the rovibrational state of N_2 recombined by ER on Ag(1 1 1) as a function of the incident projectile kinetic energy and explain it in terms of the recombination pathways at the atomic scale. Furthermore, we find a non-trivial dependence on the azimuthal angle associated with the PES topography that can lead to higher molecule yields out of the N-atoms scattering plane. The paper is organised as follows: first, the theoretical methods are described. The results and discussions section is divided into two subsections, which deal with the angular dependence and the internal energy distributions. Finally, conclusions are drawn.

2. Methodology

We have simulated the ER recombination process by means of classical MD using 3D and 6D PESs calculated by interpolation of *ab-initio* data. The technique used here for the interpolation is the corrugation reduction procedure (CRP) [36], which consists of subtracting the atom–atom interaction of the potential and interpolating the remaining energy values in order to minimise the numerical errors typically associated with interpolation of fast varying data.

The densely covered surface has been modelled *ab-initio* by a N-covered Ag(1 1 1) slab, with coverage Θ = 1, consisting of five Ag layers and N-adsorbates at the fcc sites in a (2×2) super cell. A challenging aspect of ER reaction modelling is the large configuration space spanned by the reactants. In the particular case of N-covered

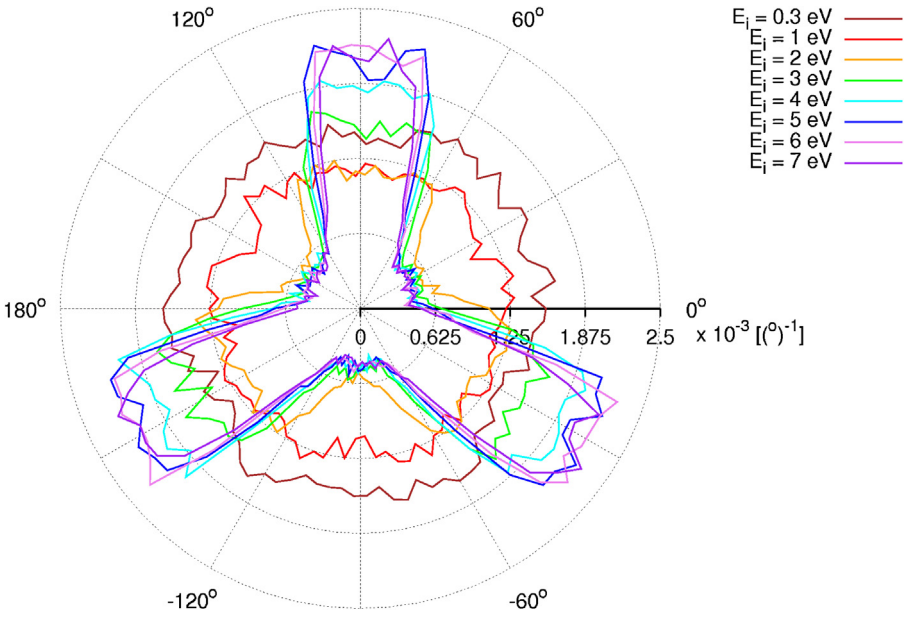

Fig. 2. Polar plot of the final azimuth, Φ_f, distribution of N_2 ER products from N(g) atoms incident at $\Theta_i = 60^\circ$ and random Φ_i values, with surface temperature $T_s = 300$ K. The distance to the plot origin indicates the desorbed N_2 intensity. Units are $(^\circ)^{-1}$, and the integral over 360° yields the efficiency for each E_i value, i.e. the number of N_2 molecules formed by ER divided by the total number of trajectories N_{traj}.

Ag(1 1 1), we need to consider the long range interaction between the atomic N projectile, labelled N(g) in the following, and the surface, as well as the motion of the adsorbed target atom, N(a), taking place during the recombination event itself. We have accounted for both effects by means of a convenient 6D PES constructed in two steps, following the procedure described in Ref. [21] and sketched in Fig. 1, which is summarised as follows: (i) For N(a)–N(g) distances larger than $R_s = 2.2$ Å we neglect the motion of the adsorbates, so that the N(g) atom follows the dynamics dictated by the 3D PES that describes its interaction with the (1×1) N-covered Ag(1 1 1) surface. The details on the construction and topography of this PES can be found in Ref. [34]. (ii) For N(a)–N(g) distances smaller than R_s we neglect adsorbates other than the target atom. In this region we use the 6D PES of a N_2 molecule interacting with clean Ag(1 1 1) [21]. Since direct pick-up reactions are the focus of the present work, the latter approach is well justified. In order to describe HA or LH processes, a higher dimensional PES would be needed to account for the motion of neighbouring adsorbed N-atoms. When integrating the classical equations of motion for N(g), it is required that the discontinuity in the force at the matching region of both PESs, defined by R_s, is as small as possible. We have verified that, using a time step $h = 0.01$ fs, the energy loss associated with this discontinuity is typically $\lesssim$2% of the E_i value [21].

Even if the recombination dynamics is overall well described within an adiabatic approach, it has been observed that the inclusion of Ag lattice vibrations as an energy loss channel in the simulations substantially improves the quantitative agreement between experimental and theoretical angular distributions of translational energies of the recombined molecules [21] and of N-atoms scattered off clean Ag(1 1 1) [37,38]. The generalized Langevin oscillator (GLO) [39–42] is used to account for lattice motion in the present work, taking previously used lattice vibrational parameters for Ag(1 1 1) [37,38,34] and keeping the surface temperature at $T_s = 300$ K.

The initial conditions for the N(g) trajectories are random lateral coordinates (x_i, y_i) and height $z_i = 6$ Å. The incident polar angle is fixed at $\Theta_i = 60^\circ$, as in the experiment [20], and a random distribution of incident azimuthal angles, Φ_i, is used. For each incident atomic energy E_i, $N_{traj} = 80,000$ trajectories are simulated. Only those resulting in ER recombination are analysed in the present work.

3. Results and discussion

3.1. Azimuth dependence

The azimuthal angle distributions of desorbing products are shown in Fig. 2 for several incident N(g) energies. Despite the random distribution of incident Φ_i values, a clear preference for outgoing $\Phi_f = -150^\circ, -30^\circ, 90^\circ$ directions is observed for $E_i > 2$ eV. These directions are parallel to the $[1\,1\,\bar{2}]$ crystallographic direction and its two equivalent directions by the surface three-fold symmetry. These three directions correspond to the top–fcc–hcp–top direction on the surface unit cell (see Fig. 1). The trajectory analysis reveals that the strong N(a)–N(g) attraction is responsible for deviating the incident projectiles on the surface plane, leading to the strongly peaked distributions of products as a function of Φ_f, observed in Fig. 2. Fig. 3 shows the Φ_f distributions of desorbing molecules corresponding to projectiles incident at given Φ_i ranges. As observed in the $E_i = 4$ eV panel, the reactive atoms incident with $\Phi_i = 60 \pm 15^\circ$, i.e. along the top-bridge direction of the unit cell (parallel to the $[\bar{1}\,1\,0]$ crystallographic direction), are strongly deviated towards the nearest N(a) adsorption fcc site, situated at $\Phi = 90^\circ$, and the desorbed molecules leave the surface with $\Phi_f \simeq 105^\circ$ and very little azimuthal spread, resulting in a narrow intensity peak. The three-fold symmetry imposes equal behaviour for atoms incident with $\Phi_i = 0 \pm 15^\circ$. For atoms incident with $\Phi_i = \pm 30 \pm 15^\circ$, the formed molecules show a broad distribution centred at an azimuth angle Φ_f equal to the incident one. Trajectories with $\Phi_i = 30 \pm 15^\circ$, i.e. along the top–hcp–fcc–top direction (parallel to $[\bar{1}\,2\,\bar{1}]$), undergo the following dynamics: the formed molecules are further scattered by the neighbouring Ag atom, i.e. they collide with the PES barrier at the last Ag top position encountered along their trajectory, so that they lose "memory" of the incident projectile trajectory and arrive at the detector with a widely spread Φ_f distribution. A similar behaviour is found for atoms incident with $\Phi_i = -30 \pm 15^\circ$. Here, however, the final collision of the product with the Ag atom leads to a somewhat narrower

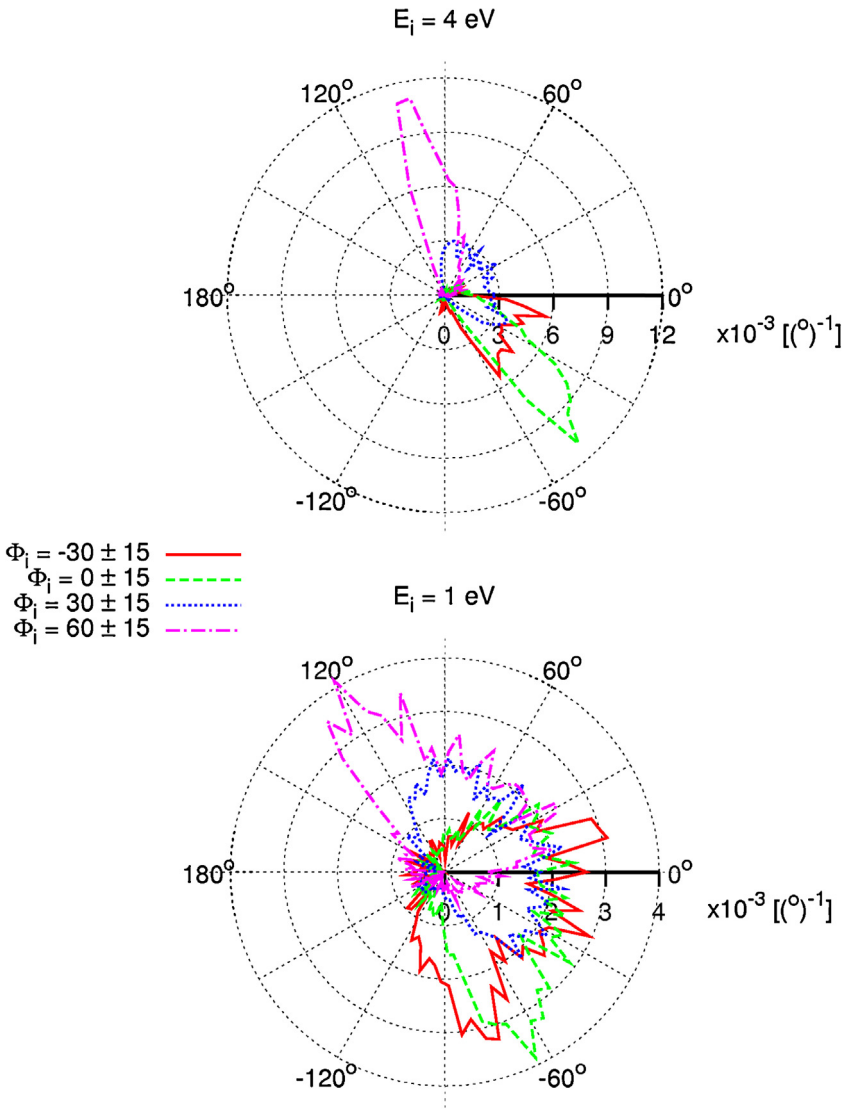

Fig. 3. Final Φ_f distribution of ER products for N(g) atoms incident at $\Theta_i = 60^\circ$ and surface temperature $T_s = 300$ K resolved for four incident Φ_i channels, as defined in Fig. 1. Top (bottom) panel is for $E_i = 4(1)$ eV. Units are $(^\circ)^{-1}$, and the integral over 360° yields the efficiency in each channel, i.e. the number of N_2 molecules formed by ER divided by the number of trajectories incident within a given channel Φ_i.

angular distribution. In summary, the aforementioned results for $\Phi_i = \pm 30 \pm 15^\circ$ channels suggest that the N_2 molecules leave the surface immediately after bond formation and they are scattered by the repulsive regions of the 6D PES. The channeling effect along azimuthal directions described above is more pronounced at high E_i values, since faster projectiles and products are less prone to lateral deflection. At small E_i values channeling is not so clear (see Fig. 3 for a comparison between the $E_i = 4$ eV and $E_i = 1$ eV cases), as the Φ_f distributions for each Φ_i channel become considerably wider.

Nevertheless, the previously discussed channeling effects lead to no enhancement of the ER reactivity for particular Φ_i directions. In other words, despite the strong dependence of the N_2 distributions on Φ_i and Φ_f, the number of formed molecules is approximately the same for every Φ_i channel. As shown in Fig. 4, the efficiency of each of the individual Φ_i channels considered above resembles the efficiency integrated for Φ_i in the $[-180^\circ, 180^\circ]$ interval for the E_i range considered here. Only the $\Phi_i = -30 \pm 15^\circ$ channel becomes less efficient than the average at large energies.

As shown by previous work, the large ER efficiency of the present system is related to the strong attractive and barrierless character of the N-covered Ag(1 1 1) PES [21], which deflects at long ranged distances the trajectories of the N(g) projectiles towards the nearest

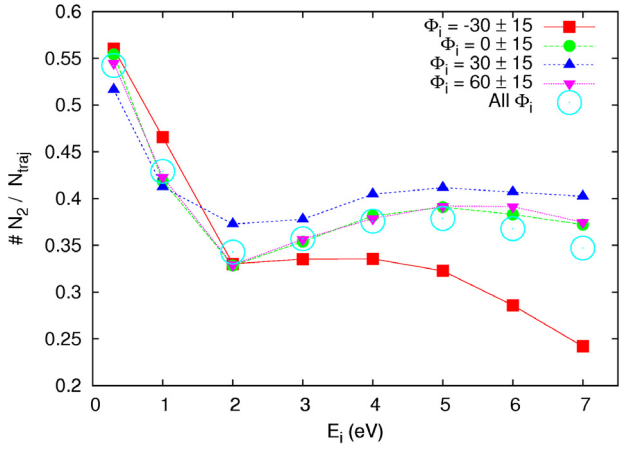

Fig. 4. Efficiency of the ER mechanism for N(g) atoms incident at $\Theta_i = 60^\circ$ and surface temperature $T_s = 300$ K resolved for several incident Φ_i channels as a function of E_i. Large symbols correspond to the average efficiency of all the incident trajectories.

N(a) adsorbate. However, once the N(g)—N(a) bond is formed, the trajectory of the products is determined by the molecule–surface interaction, which is of a strongly repulsive character [21]. In other words, the formed product seems to retain a large fraction of the deflected parallel momentum of the incident N(g) atom and then it undergoes scattering with the Ag atoms. If an Ag atom is present in the outgoing trajectory, as it is for example the case for atoms with $\Phi_i = \pm 30^\circ$ and their symmetry equivalents, the molecule will collide against it and it will be likely scattered out-of-plane. For N(g) atoms incident with $\Phi_i = 0^\circ$, 60° and their symmetry equivalents, trajectories are largely deflected before recombination, and it is very unlikely that the formed product will leave the surface within the scattering plane.

The vibrational frequency of the adsorbed N atoms obtained by DFT is 39(45) meV in the direction parallel(normal) to the surface. In the T_s = 300–600 K range, this yields a root mean square displacement of the adsorbed N-atoms $\lesssim$0.15 Å, an order of magnitude smaller than the N–N distances. Therefore, under increasing T_s, it is expected that the lobes in Fig. 2 will be broadened, but they will keep the 3-fold symmetric orientations shown there.

Summarising, the ER efficiency has a very weak angular dependence on the incident azimuth, but the outgoing azimuthal angle distributions of the formed products are strongly dependent on the incident azimuthal angles for incident N-atom energies $E_i > 2$ eV. As we have shown here, most of the molecules that originate from ER recombination tend to leave the surface at out-of-plane directions and may not be experimentally detected. This is a point that needs to be considered when interpreting the results of molecular beam experiments where just in-plane scattering is analysed.

3.2. Rovibrational states

A fundamental question in recombination reactions, not just on surfaces but also in the gas phase, is how the available energy in the system is partitioned among the degrees of freedom. In our case, the total energy to be shared is $E_{tot} = E_i + W$, where W is the energy released by N_2 formation on the surface, which amounts to 7.8 eV. This value is an estimate obtained from the calculated gas-phase N_2 molecule bond energy, which is 9.8 eV, minus the calculated N(a) adsorption energy on clean Ag(1 1 1) at the fcc site, which is 2.01 eV [38]. E_{tot} is consistent with the N-covered Ag(1 1 1) 3D PES used here, which has a global minimum of 7.43 eV at the configuration that corresponds to N_2 formation on the surface [34]. This confirms that the neighbouring adsorbed N-atoms can be neglected to a good approximation when modelling the dynamics of N_2 formation by ER and its desorption.

The average translational and rovibrational energies, $\langle E_T \rangle$ and $\langle E_{rv} \rangle$, respectively, as well as the total product energy of the formed molecules, $E_p = \langle E_T \rangle + \langle E_{rv} \rangle$, are compared to the total available energy, E_{tot}, in Fig. 5. Those energies have been calculated in the GLO (with surface temperature set to T_s = 300 K) and the adiabatic cases as averages of the energies of the molecules formed in the simulations for each E_i value. After molecule formation the energy conservation condition imposes that $E_{tot} = E_p + \langle E_{surf} \rangle$, where E_{surf} is the energy transferred into lattice motion, which is a quantity available from the GLO simulations. $\langle E_{surf} \rangle$ lies between 6 and 15% of the available E_{tot} in the studied E_i range, as shown in Fig. 5. This value is smaller than the 17–24% energy transfer to the surface calculated for N_2 formed on W(1 0 0) at E_i = 1–2.6 eV with T_s = 300–1500 K [30].

Most of the available energy for low E_i values is accounted for by the rovibrational excitation of the product. $\langle E_{rv} \rangle$ changes slightly as a function of E_i, and takes values 6.5–7 eV over the E_i range studied here. Thus, we find that there is little transfer of the N_2 formation energy into product translational energy. The fraction of energy assigned to translational motion increases almost linearly with E_i as expected for ER, but our results contrast with the findings for ER

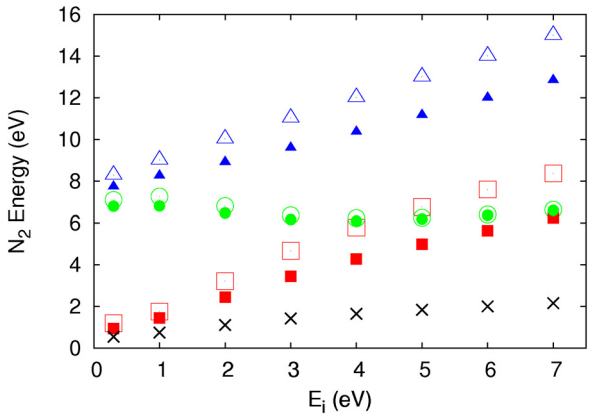

Fig. 5. Partition of the energy of the system among the available degrees of freedom after product formation as a function of the incident atom energy, E_i. Open and filled symbols correspond to the energies obtained in the adiabatic and GLO approaches, respectively, computed as average values of the products for each E_i. The surface temperature in the GLO cases is T_s = 300 K. Blue triangles are E_p, red squares are $\langle E_T \rangle$, green circles are $\langle E_{rv} \rangle$ and crosses are $\langle E_{surf} \rangle$ (see the main text for details). Note that in the adiabatic calculation E_p is equal to the total available energy, $E_{tot} = E_i + W$, when no surface temperature is considered. (For interpretation of the references to colour in this figure legend, the reader is referred to the web version of this article.)

recombination of other systems. For example, in H_2 on W(1 0 0) [15] and N_2 on W(1 0 0) [30], an increase of $\langle E_{rv} \rangle$ with E_i is noticeable. Furthermore, for H_2 and HD molecules formed on Cu(1 1 1), there is a clear conversion of the energy released in the exothermic recombination into translational energy during product formation, as translational energies ~1.3 eV have been calculated for projectiles impinging at 0.07 eV [9] in agreement with experiments [3,43]. A similar behaviour is reported for HCl formed on Au(1 1 1) [4,27,13], and H_2 and HD on Ni(1 0 0) [11].

For N_2 formed on Ag(1 1 1) at the surface temperature used in the present calculations, T_s = 300 K, the comparison of the GLO and adiabatic results shown in Fig. 5 shows that the effect of lattice vibrations is manifested only in the translational motion, i.e. the energy exchange with the surface does not affect the amount of rovibrational energy acquired by the product molecule.

In an attempt to understand the almost constant dependence of the rovibrational energy with E_i, the rovibrational term is decomposed into classical rotational ($\langle E_{rot} \rangle$) and vibrational ($\langle E_{vib} \rangle$) energies in the left panel of Fig. 6. We observe that, while the former contribution increases with E_i, the latter decreases at a rate similar to that at which $\langle E_{rot} \rangle$ increases. The behaviour of each contribution can be explained in terms of the two types of atomic mechanisms for ER recombination found previously for this system [21], which are summarised next: (i) N(g) atoms impinging with large impact parameter values, b (see Fig. 1), may react with the N(a) atom by abstracting it due to the barrierless N(g)–N(a) strong interaction. (ii) On the other hand, for small b values N(g) may enter the strongly repulsive region, force N(a) to move out of its stable position and pull it alongside when it bounces off the surface. These two mechanisms have been labelled as (i) abstraction and (ii) collision, respectively, and result in a double-peaked distribution of the b values of the reactive N(g) atoms, as shown in the inset of Fig. 6. These distributions have a feature that is important to our discussion, namely that the collision mechanism is less efficient at high E_i. At these energies, the projectile recoils with a large velocity and it is thus unable to drag the adsorbate along. However, in the energy range considered here the other mechanism is not much affected because the energy component normal to the surface, $E_i \cos^2 \Theta_i$, is much smaller than the PES attractive well depth (7.4 eV).

In our case, the "collision" mechanism results in a high vibrational excitation of the incipient molecule, as it allows for short

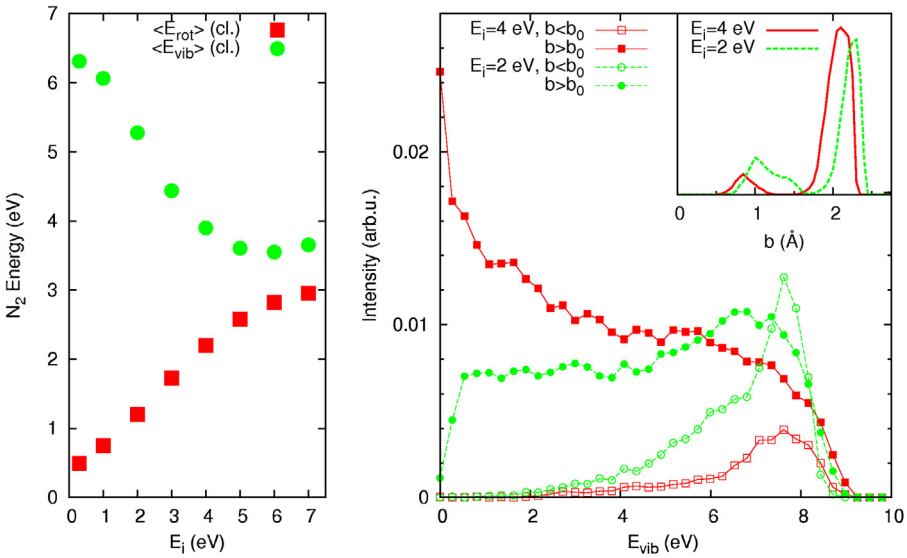

Fig. 6. Left panel: decomposition of $\langle E_{rv} \rangle$ into classical rotational and vibrational contributions as a function of E_i. Right panel: E_{vib} distributions corresponding to each product formation mechanism ("collision" or "abstraction", as explained in the main text) for $E_i = 2, 4$ eV. The mechanism assignment has been made taking reference values $b_0 = 1.7(1.5)$ Å for $E_i = 2(4)$ eV. The $b < b_0 (b > b_0)$ curves correspond to N_2 molecules formed by the "collision" ("abstraction") mechanism. The inset shows the impact parameter distribution of the reactive incident atoms for $E_i = 2, 4$ eV.

N(g)–N(a) distances, while the "abstraction" mechanism gives rise to molecules that in average are characterised by lower vibrational energies. This is precisely what we observe in the right panel of Fig. 6, where the classical vibrational energy distributions in the low ("collision") and high ("abstraction") b regimes are plotted for two representative E_i. The dip in the double peaked b value distributions can be used to define an impact parameter b_0 that distinguishes between these two regimes. The b_0 value is different for each E_i, due to the stronger deflection from their incident trajectories experienced by the less energetic projectiles, as discussed in [21]. The deflection effect is observed in the inset of Fig. 6 as a shift in the distribution toward larger b values for smaller E_i. In particular, the impact parameters used in Fig. 6 to distinguish between the two regimes are $b_0 = 1.5$ Å for $E_i = 4.0$ eV and $b_0 = 1.7$ Å for $E_i = 2.0$ eV. The decrease of $\langle E_{vib} \rangle$ as E_i increases can be explained as follows. More molecules with high vibrational excitation will be formed at lower E_i because the "collision" mechanism is more important in this energy range. As E_i increases, however, "abstraction" becomes the dominant ER recombination mechanism and therefore, the vibrational energy of the formed molecules decreases. In HCl recombination on Au(1 1 1) it has also been reported that the short b mechanism yields a narrow distribution of $\langle E_{vib} \rangle$ peaked at high energy values, whilst for the long b mechanism, which involves H–Au interaction, the distribution is broader [13].

The dependence of $\langle E_{rot} \rangle$ with E_i (see Fig. 6) can be explained in similar terms. The "abstraction" mechanism is driven by the long range character of the attractive potential and is the most efficient pathway for fast projectiles. It is expected that molecules formed by faster projectiles and high b values will have large torques, in agreement with the obtained increasing $\langle E_{rot} \rangle$ at higher E_i.

4. Conclusions

In summary, we have characterised the N_2 molecules resulting from Eley–Rideal (ER) recombination of gas-phase N atoms with the N-adsorbates of a N-covered (1×1) Ag(1 1 1) surface, with incident polar angle $\Theta_i = 60^\circ$ in the incident kinetic energy range $E_i = 0.3$–7 eV. For a random distribution of incident azimuthal angles, Φ_i, we find that the formed N_2 molecules leave the surface at preferred outgoing Φ_f azimuthal angles for $E_i > 2$ eV. A closer inspection of the $\Phi_f(\Phi_i)$ dependence shows that most products desorb at directions out of the scattering plane. Therefore, when performing molecular beam experiments, a very low ER yield might be observed if the detector is placed at an in-plane geometry. There are two factors that contribute to this pronounced azimuthal effect: (i) the long range attractive PES experienced by the atoms, which deflects projectiles towards the N adsorption site and (ii) the repulsive character of the interaction between N_2 molecules and Ag atoms, which favours scattering of the nascent product. Interestingly, despite the strong azimuth dependence of the trajectories of projectiles and products, there is little variation in the efficiency of the reaction with Φ_i.

The energy partitioning among the degrees of freedom of the formed N_2 molecules has been also characterised as a function of E_i. We observe the main features of ER products, namely: (i) highly rovibrationally excited products and (ii) average translational energies, $\langle E_T \rangle$, that increase with E_i. We find that most of the energy resulting from N—N bond formation and N—Ag bond breaking is retained by the product as rovibrational energy, in contrast with findings for other systems. Dissipation of energy into lattice vibrations accounts for <20% of the total available energy. The inclusion of this energy dissipation channel does not alter the internal product energies, but it does reduce their translational energy.

Acknowledgements

L. Martin-Gondre, P. Larrégaray and A.W. Kleyn are kindly acknowledged for stimulating discussions. This work has been supported in part by the Basque Departamento de Educación, Universidades e Investigación, the University of the Basque Country UPV/EHU (Grant No. IT-756-13), the Spanish Ministerio de Ciencia e Innovación (Grant No. FIS2010-19609-C02-02) and the European Commission (Grant No. FP7-PEOPLE-2010-RG276921). Computational resources were provided by the DIPC computing center.

References

[1] G.A. Somorjai, Introduction to Surface Chemistry and Catalysis, John Wiley and Sons, New York, 1994.
[2] K. Lykke, B.D. Kay, State-to-state inelastic and reactive molecular beam scattering from surfaces, SPIE Proc. 1208 (1990) 18.

[3] C.T. Rettner, Dynamics of the direct reaction of hydrogen atoms adsorbed on Cu(1 1 1) with hydrogen atoms incident from the gas-phase, Phys. Rev. Lett. 69 (1992) 383–386.
[4] C.T. Rettner, D.J. Auerbach, Distinguishing the direct and indirect products of a gas–surface reaction, Science 263 (1994) 365–367.
[5] C.T. Rettner, D.J. Auerbach, Dynamics of the Eley–Rideal reaction of D-atoms with H-atoms adsorbed on Cu(1 1 1). Vibrational and rotational state distributions of the HD product, Phys. Rev. Lett. 74 (1995) 4551–4554.
[6] T. Kammler, J. Lee, J. Küppers, A kinetic study of the interaction of gaseous H(D) atoms with D(H) adsorbed on Ni(1 0 0) surfaces, J. Chem. Phys. 106 (1997) 7362–7371.
[7] J.-Y. Kim, J. Lee, Spatial and kinetic separation of Eley–Rideal plus primary hot atom and secondary hot atom mechanisms in H atom abstraction of adsorbed D atoms on Pt(1 1 1), Phys. Rev. Lett. 82 (1999) 1325–1328.
[8] M. Persson, B. Jackson, Isotope effects in the Eley–Rideal dynamics of the recombinative resorption of hydrogen on a metal surface, Chem. Phys. Lett. 237 (1995) 468–473.
[9] D.V. Shalashilin, B. Jackson, M. Persson, Eley–Rideal and hot-atom reactions of H(D) atoms with D(H)-covered Cu(1 1 1) surfaces; quasiclassical studies, J. Chem. Phys. 110 (1999) 11038–11046.
[10] D. Lemoine, J.G. Quattrucci, B. Jackson, Efficient Eley–Rideal reactions of H atoms with single Cl adsorbates on Au(1 1 1), Phys. Rev. Lett. 89 (2002) 268302.
[11] Z.B. Guvenc, X. Sha, B. Jackson, Eley–Rideal and hot atom reactions between hydrogen atoms on Ni(1 0 0): electronic structure and quasiclassical studies, J. Chem. Phys. 115 (2001) 9018–9027.
[12] R. Martinazzo, S. Assoni, G. Marinoni, G.F. Tantardini, Hot-atom versus Eley–Rideal dynamics in hydrogen recombination on Ni(1 0 0). I. The single-adsorbate case, J. Chem. Phys. 120 (2004) 8761–8771.
[13] J.G. Quattrucci, B. Jackson, Quasiclassical study of Eley–Rideal and hot atom reactions of H atoms with Cl adsorbed on a Au(1 1 1) surface, J. Chem. Phys. 122 (2005) 074705.
[14] M. Bonfanti, S. Casolo, G.F. Tantardini, R. Martinazzo, Surface models and reaction barrier in Eley–Rideal formation of H_2 on graphitic surfaces, Phys. Chem. Chem. Phys. 13 (2011) 16680–16688.
[15] M. Rutigliano, M. Cacciatore, Eley–Rideal recombination of hydrogen atoms on a tungsten surface, Phys. Chem. Chem. Phys. 13 (2011) 7475–7484.
[16] M. Kori, B.L. Halpern, Vibrational energy distribution of CO in the oxidation of C on Pt, Chem. Phys. Lett. 98 (1983) 32–36.
[17] C.B. Mullins, C.T. Rettner, D.J. Auerbach, Dynamics of the oxidation of CO on Pt(1 1 1) by an atomic oxygen beam, J. Chem. Phys. 95 (1991) 8649–8651.
[18] M.C. Wheeler, D.C. Seets, C.B. Mullins, Angular dependence on the dynamic displacement of O_2 from Pt(1 1 1) by atomic oxygen, J. Chem. Phys. 107 (1997) 1672–1675.
[19] M.C. Wheeler, C.T. Reeves, D.C. Seets, C.B. Mullins, Experimental study of CO oxidation by an atomic oxygen beam on Pt(1 1 1), Ir(1 1 1), and Ru(0 0 1), J. Chem. Phys. 108 (1998) 3057–3063.
[20] H. Ueta, M.A. Gleeson, A.W. Kleyn, The interaction of hyperthermal nitrogen with N-covered Ag(1 1 1), J. Chem. Phys. 135 (2011) 074702.
[21] M. Blanco-Rey, E. Díaz, G.A. Bocan, R. Díez Muiño, M. Alducin, J.I. Juaristi, Efficient N_2 formation on Ag(1 1 1) by Eley–Rideal recombination of hyperthermal atoms, J. Phys. Chem. Lett. 4 (2013) 3704–3709.
[22] D.R. Herschbach, Molecular beam studies of internal excitation of reaction products, Appl. Opt. 4 (1965) 128–144.
[23] K.J. Laidler, Theories of Chemical Reaction Rates, McGraw-Hill, 1969.
[24] A. Hodgson, State resolved desorption measurements as a probe of surface reactions, Prog. Surf. Sci. 63 (2000) 1–61.
[25] M.J. Murphy, J.F. Skelly, A. Hodgson, Translational and vibrational energy release in nitrogen recombinative desorption from Cu(1 1 1), Chem. Phys. Lett. 279 (1997) 112–118.
[26] R.N. Carter, M.J. Murphy, A. Hodgson, On the recombinative desorption of N_2 from Ag(1 1 1), Surf. Sci. 387 (1997) 102–111.
[27] C.T. Rettner, Reaction of an H-atom beam with Cl/Au(1 1 1): dynamics of concurrent Eley–Rideal and Langmuir–Hinshelwood mechanisms, J. Chem. Phys. 101 (1994) 1529–1546.
[28] M. Blanco-Rey, J.I. Juaristi, R. Díez Muiño, H.F. Busnengo, G.J. Kroes, M. Alducin, Electronic friction dominates hydrogen hot-atom relaxation on Pd(1 0 0), Phys. Rev. Lett. 112 (2014) 103203.
[29] E. Quintas-Sánchez, P. Larrégaray, C. Crespos, L. Martin-Gondre, J. Rubayo-Soneira, J.-C. Rayez, Dynamical reaction pathways in Eley–Rideal recombination of nitrogen from W(1 0 0), J. Chem. Phys. 137 (2012) 064709.
[30] E. Quintas-Sánchez, C. Crespos, P. Larrégaray, J.-C. Rayez, L. Martin-Gondre, J. Rubayo-Soneira, Surface temperature effects on the dynamics of N_2 Eley–Rideal recombination on W(1 0 0), J. Chem. Phys. 138 (2013) 024706.
[31] J.C. Tully, Dynamics of gas–surface interactions: reaction of atomic oxygen with adsorbed carbon on platinum, J. Chem. Phys. 73 (1980) 6333–6342.
[32] R. Martinazzo, G.F. Tantardini, Quantum study of Eley–Rideal reaction and collision induced desorption of hydrogen atoms on a graphite surface. I. H-chemisorbed case, J. Chem. Phys. 124 (2006) 124702.
[33] R. Martinazzo, G.F. Tantardini, Quantum study of Eley–Rideal reaction and collision induced desorption of hydrogen atoms on a graphite surface. I. H-physisorbed case, J. Chem. Phys. 124 (2006) 124703.
[34] M. Blanco-Rey, L. Martin-Gondre, R. Díez Muiño, M. Alducin, J.I. Juaristi, Dynamics of nitrogen scattering off N-covered Ag(1 1 1), J. Phys. Chem. C 116 (2012) 21903–21912.
[35] T. Zaharia, H. Ueta, A.W. Kleyn, M.A. Gleeson, Nitrogen scattering at Ru(0 0 0 1) surfaces, Z. Phys. Chem. 227 (2013) 1511–1522.
[36] H.F. Busnengo, A. Salin, W. Dong, Representation of the 6D potential energy surface for a diatomic molecule near a solid surface, J. Chem. Phys. 112 (2000) 7641–7651.
[37] L. Martin-Gondre, M. Alducin, G.A. Bocan, R. Díez Muiño, J.I. Juaristi, Competition between electron and phonon excitations in the scattering of nitrogen atoms and molecules off tungsten and silver metal surfaces, Phys. Rev. Lett. 108 (2012) 096101.
[38] L. Martin-Gondre, G.A. Bocan, M. Blanco-Rey, M. Alducin, J.I. Juaristi, R. Díez Muiño, Scattering of nitrogen atoms off Ag(1 1 1) surfaces: a theoretical study, J. Phys. Chem. C 117 (2013) 9779–9790.
[39] S.A. Adelman, J.D. Doll, Generalized Langevin equation for atom-solid-surface scattering. General formulation for classical scattering off harmonic solids, J. Chem. Phys. 64 (1976) 2375–2388.
[40] S.A. Adelman, Generalized Langevin theory for many-body problems in chemical dynamics. General formulation and the equivalent harmonic chain representation, J. Chem. Phys. 71 (1979) 4471–4486.
[41] J.C. Tully, Dynamics of gas–surface interactions. 3D generalized Langevin model applied to fcc and bcc surfaces, J. Chem. Phys. 73 (1980) 1975–1985.
[42] H.F. Busnengo, M.A. Di Césare, W. Dong, A. Salin, Surface temperature effects in dynamic trapping mediated sdsorption of light molecules on metal surfaces: H_2 on Pd(1 1 1) and Pd(1 1 0), Phys. Rev. B 72 (2005) 125411.
[43] C.T. Rettner, D.J. Auerbach, Dynamics of the formation of HD from D(H) atoms colliding with H(D)/Cu(1 1 1): a model study of an Eley–Rideal reaction, Surf. Sci. 357 (1996) 602–608.